



Fungal Parasite Transmission in a Planktonic Ecosystem Under Light and Nutrient Constraints

Yawen Yan^{1,3} · Juping Ji^{2,3} · Hao Wang³

Received: 15 April 2024 / Accepted: 24 September 2024 / Published online: 13 October 2024
© The Author(s), under exclusive licence to the Society for Mathematical Biology 2024

Abstract

The two main components of the planktonic ecosystem are phytoplankton and zooplankton. Fungal parasites can infect zooplankton and spread between them. In this paper, we construct a dynamic model to describe the spread of fungal parasites among zooplankton. Basic reproduction number for fungal parasite transmission among zooplankton are rigorously derived. The dynamics of this system are analyzed including dissipativity and equilibria. We further explore the effects of ecological factors on population dynamics and the relationship between fungal parasite transmission and phytoplankton blooms. Interestingly, our theoretical and numerical results indicate that a low-light or oligotrophic aquatic environment is helpful in mitigating the transmission of fungal parasites. We also show that fungal parasites on zooplankton can increase phytoplankton biomass and induce blooms.

Keywords Dynamic model · Light and nutrient · Fungal parasite transmission · Phytoplankton bloom · Ecological factors

Mathematics Subject Classification 92D25 · 92B05

Yan is supported by Harbin Engineering University PhD Scholarship; Ji is supported by National Natural Science Foundation of P. R. China (No. 12401635) and Science and Technology Program of Guangzhou City (202201020546); Wang is supported by the Natural Sciences and Engineering Research Council of Canada (Individual Discovery Grant RGPIN-2020-03911 and Discovery Accelerator Supplement Award RGPAS-2020-00090).

✉ Juping Ji
juping@gzhu.edu.cn

- ¹ School of Mathematical Sciences, Heilongjiang University, Harbin, Heilongjiang 150080, P.R. China
- ² School of Mathematics and Information Sciences, Guangzhou University, Guangzhou, Guangdong 510006, P.R. China
- ³ Department of Mathematical and Statistical Sciences, University of Alberta, Edmonton, Alberta T6G 2G1, Canada

1 Introduction

Planktonic ecosystems have two primary components: phytoplankton and zooplankton (Hall et al. 2009). Phytoplankton form the foundation of the planktonic ecosystem. Their growth requires two essential resources: light and nutrients (Zhao et al. 2020; Peace 2015; Huisman et al. 2006; Klausmeier and Litchman 2001; Wang et al. 2007; Zhang et al. 2023). Light entering the water column is absorbed by the water and other substances, and its intensity decreases exponentially as the depth increases (Peace 2015; Huisman and Weissing 1994; Pang et al. 2019; Peng and Zhao 2016). Nutrients primarily originate from sediment, which is transported to the aquatic habitat through water exchange and turbulence (Klausmeier and Litchman 2001; Yu et al. 2019). Phytoplankton use light energy to transform carbon dioxide and water into organic matter while releasing oxygen (Davies and Wang 2021). Simultaneously, they ingest various nutrients from the surrounding environment to sustain their growth and reproduction. These processes are pivotal for the natural energy conversion, element cycling, and maintenance of the atmospheric carbon-oxygen balance (Zhao et al. 2020). Zooplankton is a significant part of planktonic ecosystems. They graze on phytoplankton and transfer energy and nutrients to higher trophic levels (Chen et al. 2022; Müller-Navarra et al. 2000). As a result, zooplankton can regulate the abundance of phytoplankton and impact the health and stability of the aquatic ecosystem.

Fungal parasites are important heterotrophic microbial eukaryotes that exist in aquatic environments in the form of free-living spores (Shocket et al. 2018; Civitello et al. 2013; Cáceres et al. 2014; Chen et al. 2024). As parasites, free-living fungal spores attack aquatic organisms and influence the structure of the food web (Kagami et al. 2007). Some fungal parasites exhibit parasitic relationships with zooplankton. For example, the fungal parasite *Metschnikowia bicuspidata* parasitizes *Daphnia dentifera* (Shocket et al. 2018; Strauss et al. 2015; Cáceres et al. 2014; Civitello et al. 2013). Therefore, fungal parasites can directly affect the structure and dynamics of planktonic ecosystems.

In this study, we consider fungal parasites infecting zooplankton. The parasitic process of fungi can be divided into the following stages. In the first stage, fungal parasites move freely in water as spores. These spores are distributed in the phytoplankton habitat (Civitello et al. 2013; Hall et al. 2007). Zooplankton can accidentally ingest fungal spores when feeding on phytoplankton. The second stage is that fungal spores replicate and reproduce in the zooplankton gut and eventually fill the entire body cavity. In the final stage, when infected zooplankton die, the fungal spores in their bodies are released into the water (Shocket et al. 2018). The process indicates that fungal parasites cause zooplankton death and reduce their biomass. Many researchers have modeled the spread of fungal parasites among zooplankton (Cáceres et al. 2014; Strauss et al. 2015; Shocket et al. 2018; Hall et al. 2007, 2009). Hall et al. (Hall et al. (2007)) investigated the connection between foraging ecology and disease transmission in a zooplankton-fungal system. Cáceres et al. (Cáceres et al. (2014)) explored the impact of dilution effect on the fungal parasite transmission in focal hosts. Shocket et al. (Shocket et al. (2018)) discussed the impact of climatic warming on infectious diseases and proposed a mechanistic framework to predict different temperature-disease outcomes. Strauss et al. (Strauss et al. (2015)) explored the dilution effect among competitors using an

eco-epidemiological model, considering factors such as species densities, assembly order, and competence. These models mentioned above do not consider that the growth of phytoplankton requires light and nutrients. Experimental studies have revealed that light intensity and nutrients have significant impacts on phytoplankton (Huisman et al. 2006; Klausmeier and Litchman 2001).

Motivated by the above discussion and excellent work, we propose a dynamic model to describe fungal parasite transmission among zooplankton. This model contains phytoplankton, zooplankton, and fungal parasites. An important feature of our model compared to previous models is the consideration of light and nutrients. One principal objective of the present paper is to show the effects of light and nutrients on the spread of fungal diseases. We will rigorously derive the basic reproduction number for fungal parasite transmission by analyzing dynamics of the model.

Phytoplankton blooms are seriously harmful to aquatic ecosystems. The toxins produced by phytoplankton can accumulate in aquatic food webs, causing disease and even death in aquatic organisms and humans. Additionally, frequent phytoplankton blooms can deplete the oxygen in the water, leading to the death of aquatic organisms and ultimately causing an imbalance and collapse of the entire aquatic ecosystem. Another objective of this study is to explore the relationship between fungal parasite transmission and phytoplankton blooms.

The structure of this paper is as follows. In sect. 2, we establish a dynamic model to describe the interactions among phytoplankton, zooplankton and fungal parasites in a well-mixed water column. In sect. 3, we analyze dynamic properties of the model including dissipativity and equilibria, and establish the basic reproduction number of fungal parasite transmission among zooplankton. By using numerical bifurcation diagrams and time series diagrams, we explore the effects of ecological factors on population dynamics and the relationship between fungal parasite transmission and phytoplankton blooms in sect. 4. The final section summarizes the main conclusions and presents some future works.

2 Model Formulation

We develop a dynamic model to describe the interactions among phytoplankton, zooplankton and fungal parasites in a well-mixed water column. The growth of phytoplankton depends on light and nutrients. Fungal parasites move freely in water as spores. Zooplankton consume phytoplankton and accidentally ingest fungal spores. Let x denote the depth of the water column, where $x = 0$ and $x = x_l$ correspond to the water surface and bottom, respectively. The model contains five nonlinear ordinary differential equations that describe the rate of change for phytoplankton (P), susceptible zooplankton (S), infected zooplankton (I), fungal parasites (F) and dissolved nutrients (N). Their interaction relationships are shown in Fig. 1. All the variables and parameters of the model and their biological significance are presented in Table 1.

According to the research work in Strauss et al. (2015); Cáceres et al. (2014); Shocket et al. (2018), we have the following assumptions:

- (A1) The parasites are horizontally transmitted.

Table 1 Variables and parameters of system (1)

Symbol	Meaning	Values	Units	Source
t	Time	Variables	day	
x	Depth	Variables	m	
P	Biomass density of phytoplankton	Variables	mg C/m ³	
S	Biomass density of susceptible zooplankton	Variables	mg C/m ³	
I	Biomass density of infected zooplankton	Variables	mg C/m ³	
F	Density of fungal parasites in water	Variables	spores/m ³	
N	Concentration of dissolved nutrients	Variables	mg P/m ³	
r	Maximum specific production rate of phytoplankton	1	day ⁻¹	(Strauss et al. 2015; Yan et al. 2022b)
d_p	Loss rate of phytoplankton	0.06	day ⁻¹	Assumption
d_z	Loss rate of zooplankton	0.04	day ⁻¹	Assumption
d_f	Loss rate of fungal parasites	0.08	day ⁻¹	Assumption
L_0	Light intensity at the water surface	300	μmol(photons)/(m ² s)	(Yan et al. 2022b, a; Wang et al. 2007)
l_0	Background light attenuation coefficient	0.54(0.3–0.9)	m ⁻¹	(Wang et al. 2007)
l	Light attenuation coefficient of phytoplankton	0.0003	m ² /mg C	(Wang et al. 2007)
h	Half saturation constant for light-limited production of phytoplankton	100	μmol(photons)/(m ² s)	(Yan et al. 2022a)
γ	Half saturation constant for nutrient-limited production of phytoplankton	3	mg P/m ³	(Yan et al. 2022a)
a	Zooplankton foraging rate	0.0045	(mg C/m ³) ⁻¹ day ⁻¹	Assumption
e	Zooplankton conversion rate	0.6	–	(Chen et al. 2017)
ρ	Fecundity reduction due to infection	0.9	–	(Cáceres et al. 2014)
β	Per fungal spore infectivity	0.17	spore ⁻¹	Assumption
q	Maximal spore yield	12	spores/mg C	Assumption
δ	Lytic death rate	0.48	day ⁻¹	(Shocket et al. 2018)
θ	Half saturation constants of $\sigma(P)$	10	mg C/m ³	(Shocket et al. 2018)
N_0	Nutrient input from the bottom of water column	120(0-500)	mg P/m ³	(Wang et al. 2007)
c_p	Nutrient to carbon quotas of phytoplankton	0.015(0.004–0.04)	mg P/mg C	(Yan et al. 2022a)
D	Water exchange rate	0.02	m/day	(Wang et al. 2007)
x_l	Depth of the water column	10	m	Assumption

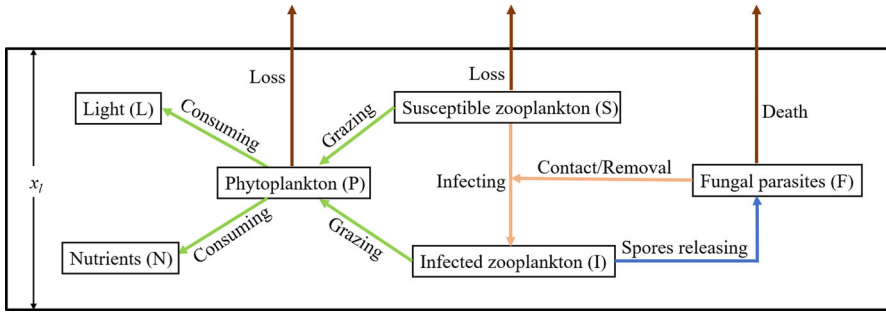


Fig. 1 Phytoplankton-zooplankton-fungal parasites interactions in a well-mixed water column

(A2) Fungal spores only release from dead infected zooplankton.

Phytoplankton growth is limited by several abiotic factors. We assume that it primarily relies on the availability of light intensity $L(x, P)$ and nutrient concentration (N) . The light intensity $L(x, P)$ at a depth x , following the Lambert-Beer law (Huisman and Weissing 1994), is given by

$$L(x, P) = L_0 \exp(-l_0x - lPx), x \in (0, x_l).$$

For light-limited phytoplankton growth, we use the Monod function (Wang et al. 2007; Klausmeier and Litchman 2001), denoted as

$$f(P) = \frac{1}{x_l} \int_0^{x_l} \frac{L(x, P)}{h + L(x, P)} dx,$$

here h is the half saturation constant. As for the expression of nutrient, we also use the Monod function (Wang et al. 2007; Klausmeier and Litchman 2001)

$$g(N) = \frac{N}{\gamma + N},$$

where γ is the half saturation constant. The growth rate of phytoplankton is represented by $rg(N)f(P)P$. The reduction of phytoplankton is due to natural mortality and respiration $(d_p P)$, and predation by zooplankton $(\pi_1(P)(S + I))$.

Zooplankton is divided into two classes: susceptible zooplankton (S) and infected zooplankton (I) . By Assumption (A1), the increase of susceptible zooplankton comes from the reproduction of susceptible and infected zooplankton (Cáceres et al. 2014; Shocket et al. 2018). But the fertility rate of infected zooplankton decreases with the proportion $\rho \in [0, 1)$. Moreover, susceptible and infected zooplankton consume phytoplankton with a conversion rate e . The reduction of susceptible zooplankton has two parts. One is natural mortality and respiration $(d_z S)$, and the other is infected by fungal parasites $(\beta\pi_2(F)S)$. The changes in infected zooplankton biomass include the infection $\beta\pi_2(F)S$, natural mortality and respiration $d_z I$, and lytic death δI .

Previous studies have shown that the number of fungal spores released after the death of infected zooplankton depends on phytoplankton (Hall et al. 2009). It is assumed to be $\delta\sigma(P)I$. Fungal spores are removed by zooplankton with $\pi_2(F)(S+I)$. The changes of dissolved nutrients N depend on the consumption of phytoplankton $c_p r g(N)f(P)P$ and the exchange of nutrients $(D/x_l)(N_0 - N)$ at the bottom of the water column.

Based on the above assumptions and formulations, we construct the following phytoplankton-zooplankton-fungal parasite model

$$\begin{aligned} \frac{dP}{dt} &= r g(N)f(P)P - d_p P - \pi_1(P)(S + I), \\ \frac{dS}{dt} &= e\pi_1(P)(S + \rho I) - d_z S - \beta\pi_2(F)S, \\ \frac{dI}{dt} &= \beta\pi_2(F)S - d_z I - \delta I, \\ \frac{dF}{dt} &= \delta\sigma(P)I - d_f F - \pi_2(F)(S + I), \\ \frac{dN}{dt} &= \frac{D}{x_l}(N_0 - N) - c_p r g(N)f(P)P. \end{aligned} \tag{1}$$

According to Strauss et al. (2015), Cáceres et al. (2014), and Shocket et al. (2018), we assume that the functions

$$\pi_1(P) = aP, \quad \pi_2(F) = aF, \quad \sigma(P) = \frac{qP}{\theta + P}.$$

Considering the biological implications of this model, we will explore the solutions of (1) with initial values

$$P(0) \geq 0, S(0) \geq 0, I(0) \geq 0, F(0) \geq 0, N(0) \geq 0. \tag{2}$$

3 Model Dynamics

In this section, we investigate the dynamical properties of model (1) containing dissipation, as well as the existence and stability of equilibria. By standard mathematical arguments, model (1) has a unique nonnegative global solution for any initial values satisfying (2). Let

$$\Omega := \left\{ (P, S, I, F, N) \in \mathbb{R}_+^5 \mid P \geq 0, S \geq 0, I \geq 0, F \geq 0, N \geq 0 \right\}.$$

and $B = erg(N_0)f(0)A / \min\{d_p, d_z\}$, where A satisfies the condition $rg(N_0)f(A) = d_p$.

We first show that system (1) is dissipative. The proof can be found in Appendix A.

Theorem 3.1 *The set*

$$\Delta := \left\{ (P, S, I, F, N) \in \Omega \mid N \leq N_0, (eP + S + I) \leq \frac{erg(N_0)f(0)A}{\min\{d_p, d_z\}}, F \leq \frac{\delta\sigma(A)B}{d_f} \right\}$$

is a globally attracting region, which means that system (1) is dissipative.

In order to study the spread of fungal parasites in zooplankton, we investigate the dynamics of system (1). Model (1) has four possible equilibria:

- (1) Nutrient-only equilibrium $E_0 = (0, 0, 0, 0, N_0)$;
- (2) Phytoplankton-nutrient equilibrium $E_1 = (P_1, 0, 0, 0, N_1)$, where P_1 and N_1 are the solution of

$$\begin{aligned} rg(N)f(P) - d_p &= 0, \\ \frac{D}{x_l}(N_0 - N) - c_p rg(N)f(P)P &= 0; \end{aligned} \tag{3}$$

- (3) Disease-free equilibrium $E_2 = (P_2, S_2, 0, 0, N_2)$, where P_2, S_2, N_2 are solved by

$$rg(N)f(P)P - d_p P - \pi_1(P)S = 0, \tag{4}$$

$$e\pi_1(P) - d_z = 0, \tag{5}$$

$$\frac{D}{x_l}(N_0 - N) - c_p rg(N)f(P)P = 0; \tag{6}$$

- (4) Endemic equilibrium $E_3 = (P_3, S_3, I_3, F_3, N_3)$, where $P_3, S_3, I_3, F_3,$ and N_3 are determined by solving

$$\begin{aligned} rg(N)f(P)P - d_p P - \pi_1(P)(S + I) &= 0, \\ e\pi_1(P)(S + I) - d_z S - \beta\pi_2(F)S &= 0, \\ \beta\pi_2(F)S - d_z I - \delta I &= 0, \\ \sigma(P)\delta I - d_f F - \pi_2(F)(S + I) &= 0, \\ \frac{D}{x_l}(N_0 - N) - c_p rg(N)f(P)P &= 0. \end{aligned}$$

To facilitate the following analysis, we define the critical values as

$$d_p^* = rg(N_0)f(0), d_z^* = eaP_1, \bar{d}_p = rg(N_2)f(P_2). \tag{7}$$

For the equilibria E_0, E_1, E_2 and E_3 , we have the following theoretical results. The proof can be found in [Appendix B.1](#), [Appendix B.2](#), [Appendix B.3](#), and [Appendix B.4](#).

Theorem 3.2 E_0 always exists and it is globally asymptotically stable if $d_p > d_p^*$, while E_0 is unstable if $d_p < d_p^*$.

Theorem 3.3 E_1 exists uniquely if and only if $d_p < d_p^*$, and it is locally asymptotically stable if $d_z > d_z^*$.

According to the approach of the next-generation matrix in Van den Driessche and Watmough (2002), we define the second-order vectors corresponding to equations I and F as

$$\mathcal{G} = \begin{pmatrix} \beta\pi_2(F)S \\ 0 \end{pmatrix},$$

$$\mathcal{V} = \begin{pmatrix} d_z I + \delta I \\ -\delta\sigma(P)I + d_f F + \pi_2(F)(S + I) \end{pmatrix}.$$

At the disease-free equilibrium $E_2 = (P_2, S_2, 0, 0, N_2)$, the Jacobian matrices of \mathcal{G} and \mathcal{V} are

$$G = \begin{pmatrix} 0 & \beta a S_2 \\ 0 & 0 \end{pmatrix}, \quad V = \begin{pmatrix} d_z + \delta & 0 \\ -\delta\sigma(P_2) & d_f + a S_2 \end{pmatrix}.$$

Therefore, the next generation matrix is

$$GV^{-1} = \begin{pmatrix} \frac{\beta a S_2 \delta \sigma(P_2)}{(d_f + a S_2)(d_z + \delta)} & \frac{a S_2}{d_f + a S_2} \\ 0 & 0 \end{pmatrix}.$$

The basic reproduction number R_0 is calculated as the spectral radius of the next generation matrix GV^{-1} . It is expressed as

$$R_0 = \frac{\beta a S_2 \delta \sigma(P_2)}{(d_f + a S_2)(d_z + \delta)}. \tag{8}$$

From (5), we obtain $P_2 = d_z/ea$, and then $\sigma(P_2) = \frac{qd_z}{d_z + \theta ea}$. As a result, the expression of (8) can be further simplified to

$$R_0 = \frac{\beta a S_2 \delta q d_z}{(d_f + a S_2)(d_z + \delta)(d_z + ea\theta)}. \tag{9}$$

The index R_0 measures the transmission capacity of fungal parasites. $R_0 < 1$ means that fungal parasites go extinct. $R_0 = 1$ is a critical value that determines whether fungal parasites can invade an aquatic ecosystem.

Remark 3.4 1. Note that $R_0 < 1$ if $\beta q < 1$, which implies that if the infectivity is low or the spore yield is minimal, the fungal parasites may not spread.
 2. There are nonlocal terms in (4) and (6), which make it difficult for us to obtain the specific expression of S_2 and theoretically obtain the evolution trends of R_0 with respect to the parameters. However, from the structure of equations (4), (6) and (9), we find that R_0 is related to fungal infection-related parameters (β, q, δ), resource-related factors (L_0, l_0, l, N_0, D, c_p), and other factors ($x_l, a, e, r, d_p, d_z, d_f$).

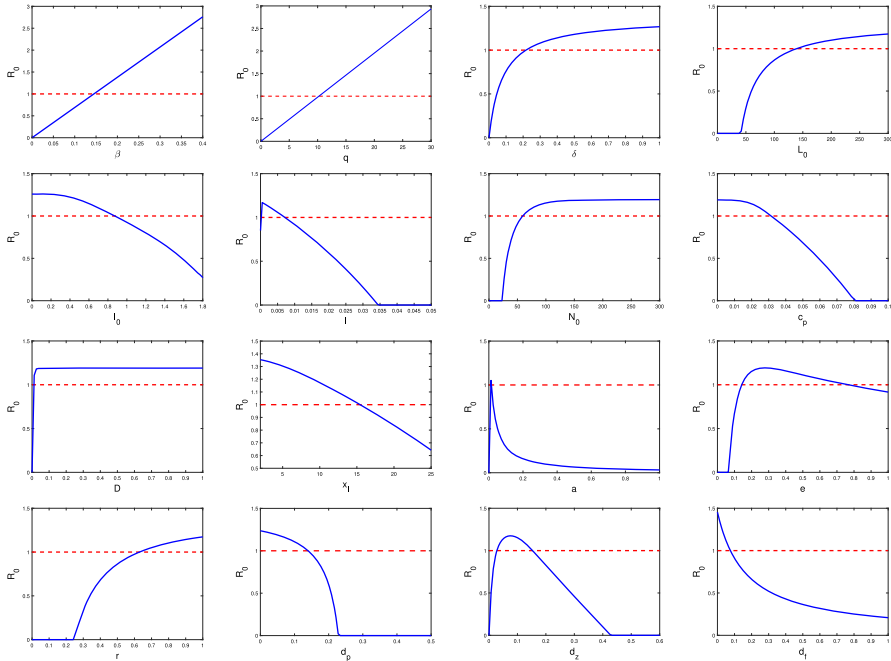


Fig. 2 Dependence of R_0 on some model parameters. Here $L_0 = 300$, $N_0 = 120$ and the remaining parameter values are derived from Table 1

3. Figure 2 reveals that high β , q , δ , L_0 , N_0 , D and r are conducive to fungal disease transmission, while high l_0 , x_1 , d_p and d_f prevent fungal parasites invasion. The dependence of R_0 on l , e , d_z is complicated. Both high and low l , e , d_z may be detrimental to the survival of fungi.

Theorem 3.5 E_2 exists if and only if $d_p < \bar{d}_p$. Moreover, if $R_0 < 1$, then E_2 is locally asymptotically stable, otherwise E_2 is unstable.

We next prove the existence of E_3 with d_f as the bifurcation parameter. Define

$$d_f^* = aS_2 \left(\frac{\beta\delta\sigma(P_2)}{\delta + d_z} - 1 \right).$$

We will show that E_3 bifurcates from E_2 at $d_f = d_f^*$ using bifurcation theory in Crandall and Rabinowitz (1971); Shi and Wang (2009).

Theorem 3.6 If $R_0 > 1$ holds, then (1) has at least one endemic equilibrium E_3 for $0 < d_f < d_f^*$.

Figure 3 shows the extinction-survival spectrum of phytoplankton, zooplankton, and fungal spores in the (d_p, d_z) -plane. In Δ_0 , the solutions of (1) converge to E_0 , which implies the extinction of all three species (see Fig. 4a). This indicates that if phytoplankton is extinct, zooplankton and fungal parasites will not survive. Phytoplankton

Fig. 3 Parameter regions of d_p versus d_z for the survival and extinction of phytoplankton, zooplankton and fungal parasite. Three species go extinct in Δ_0 , phytoplankton survive while zooplankton and fungal parasite are extinct in Δ_1 , susceptible zooplankton successfully invade aquatic habitats, while fungal parasite cannot survive in Δ_2 , fungal parasite transmission among zooplankton as equilibria or periodic solutions form in Δ_3 . The remaining parameters are from Table 1

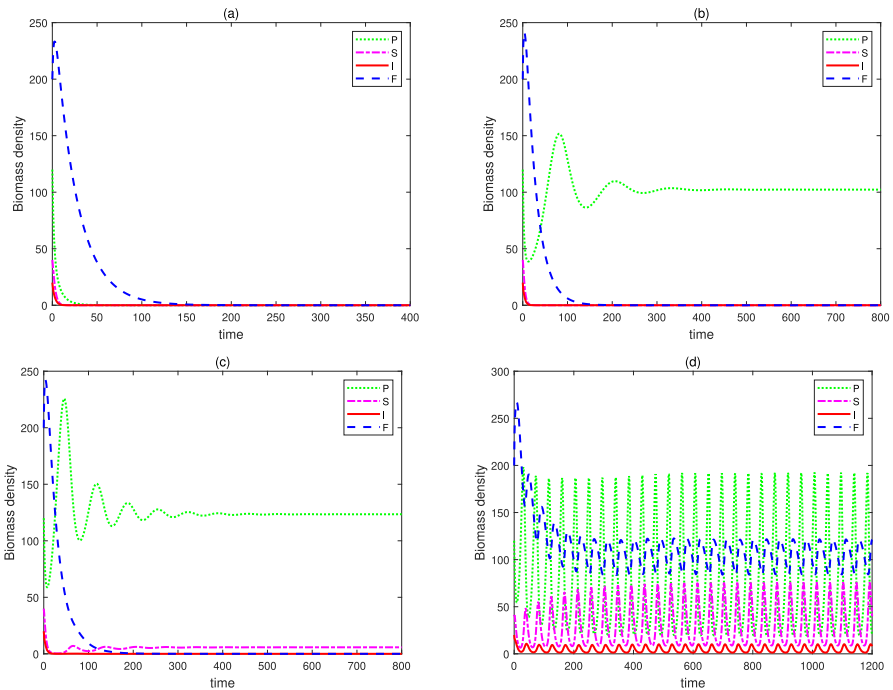
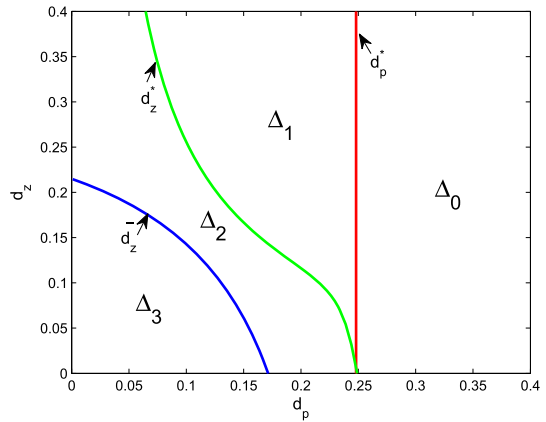


Fig. 4 Time series of attractor regions. **a** Δ_0 region: $d_p = 0.3, d_s = 0.3$; **b** Δ_1 region: $d_p = 0.15, d_s = 0.2$; **c** Δ_2 region: $d_p = 0.1, d_s = 0.2$; **d** Δ_3 region: $d_p = 0.03, d_s = 0.06$. The remaining parameters are from Table 1

survive in Δ_1 and the solutions of model (1) converge to E_1 if $(d_p, d_z) \in \Delta_1$ (see Fig. 4b). Within Δ_2 , phytoplankton and susceptible zooplankton appear together and the solutions of (1) converge to E_2 when $(d_p, d_z) \in \Delta_2$ (see Fig. 4c). Phytoplankton, zooplankton, and fungal parasites can coexist in Δ_3 , and the solutions of (1) converge to E_3 or positive periodic solutions if $(d_p, d_z) \in \Delta_3$ (see Fig. 4d).

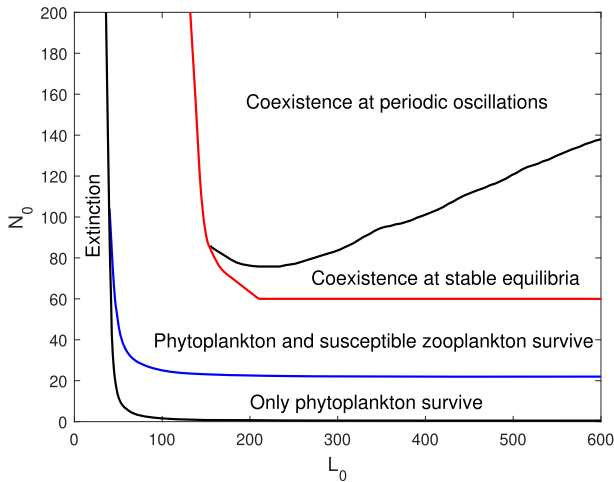


Fig. 5 Parameter regions of L_0 versus N_0 describe the survival and extinction of phytoplankton, zooplankton and fungal parasites

Due to the occurrence of a Hopf bifurcation, positive equilibrium E_3 loses its stability there, and a positive periodic solution emerges. This means that fungal parasites spread between zooplankton in the form of periodic oscillation. The positive periodic solution is a very important dynamic behavior. However, because the model is a high-dimensional ordinary differential equation system, it is difficult to give a theoretical proof of the occurrence of Hopf bifurcation and the existence of positive periodic solutions.

4 Effect of Ecological Factors

Ecological factors have an important influence on biological communities. In this section, we will carry out some numerical simulations to explore how the system (1) responds to the ecological factors. We mainly focus on the effects of light and nutrients on fungal parasite transmission and explore the relationship between fungal parasite transmission and phytoplankton blooms through bifurcation diagrams and time series diagrams.

We consider the roles of light and nutrients in fungal parasite transmission. Surface light intensity L_0 and nutrient input concentration N_0 are important parameters related to light and nutrients, respectively. Thus, we use these two parameters as factors to study fungal parasite transmission. Figure 5 shows the combined effect of L_0 and N_0 on the survival and extinction of all species. One can observe that all species become extinction under low L_0 and N_0 . With the increase of L_0 and N_0 , phytoplankton invades aquatic ecosystems. When L_0 and N_0 cross from the blue line to the next area, susceptible zooplankton invade and coexist with phytoplankton in an aquatic environment. Once L_0 and N_0 exceed the red line, the fungal parasites begin to spread among zooplankton as a stable equilibria form or as a periodic solution form (see

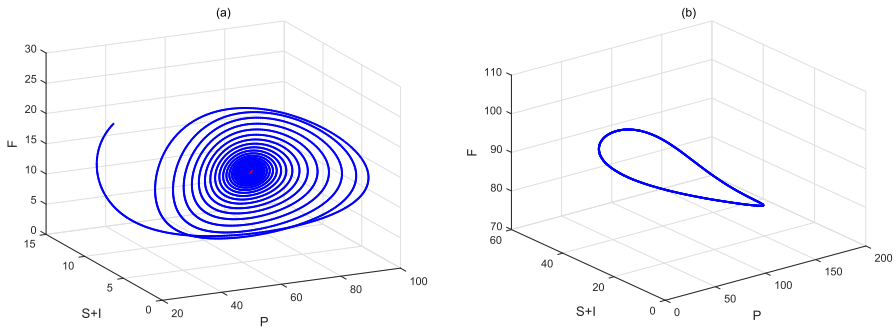


Fig. 6 The phase portraits of system (1). **a** The system has a stable endemic equilibrium for $L_0 = 150$ and $N_0 = 80$. **b** The system exhibits periodic oscillations for $L_0 = 300$ and $N_0 = 120$. The remaining parameter values are shown in Table 1

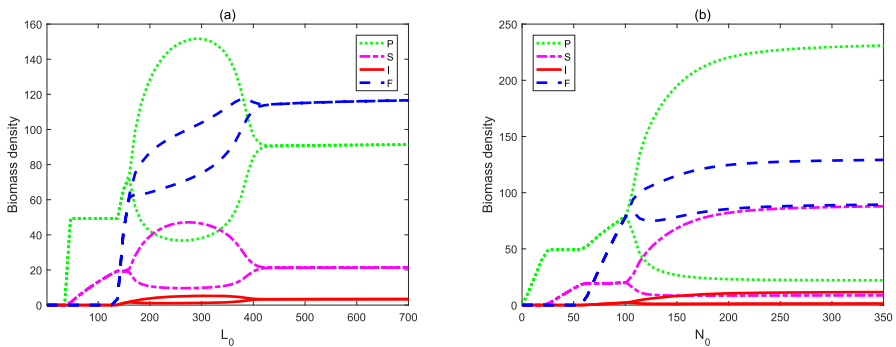


Fig. 7 Influence of the sediment input nutrient concentration N_0 and water surface light intensity L_0

Fig. 6). These results indicate that fungal parasites are difficult to spread in a low-light or oligotrophic aquatic ecosystem.

To better understand the effects of light and nutrients on the spread of fungal parasites, we now consider bifurcation diagrams for all populations with respect to L_0 or N_0 . Figure 7a shows that very low light intensity causes the extinction of all species. As L_0 increases, the infection of fungal parasites gradually prevails in aquatic ecosystems. During this progress, there are two stability switches from a stable equilibrium to periodic oscillation and then back to a stable equilibrium. When L_0 is beyond a certain extent, population biomass is almost unchanged, which indicates that high L_0 has little effect on the spread of fungal parasites. Figure 7b demonstrates that fungal parasites cannot spread among zooplankton when N_0 is low. With a further increase of N_0 , fungal parasites spread among zooplankton with a stable equilibrium and a stable periodic solution. These findings also indicate that the changes in light and nutrients cause the transmission of fungal parasites.

Light intensity varies with the seasons (see Fig. 8). It is well worthwhile to compare the effects of seasonal and constant light intensity on the spread of fungal parasites. The bifurcation diagrams in Figs. 9a–d and 10a–d show the changes in population dynamics with parameters β and q , and also compare the impact of constant light intensity

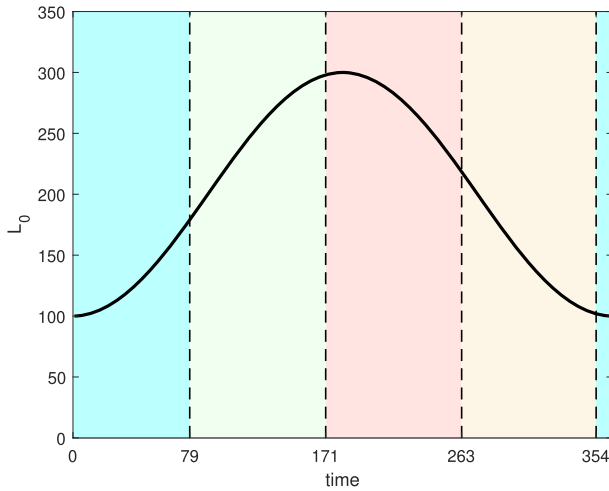


Fig. 8 Seasonal fluctuations in light intensity $L_0(t) = 200 \times [1.0 - 0.5 \cos(2\pi t/365)]$, $t=365$ days. The horizontal axis represents the number of days and corresponds to specific dates in the four seasons. Days 79 to 171 represent spring, with June 22nd being the corresponding date for day 79. The period from 171 to 263 days represents summer, with September 23rd being the corresponding date for day 171. Days 263 to 354 represent autumn, with December 22nd being the corresponding date for day 263. Finally, days 354 to 79 represent winter, with March 21st of the following year being the corresponding date for day 79

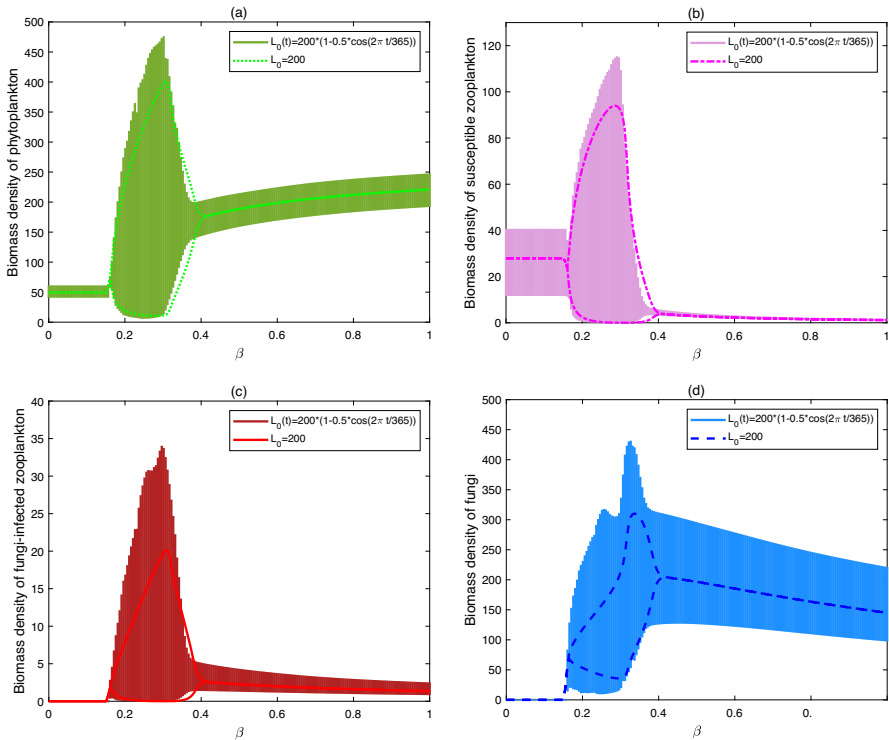


Fig. 9 Influence of the transmission coefficient β under constant or seasonal light intensity

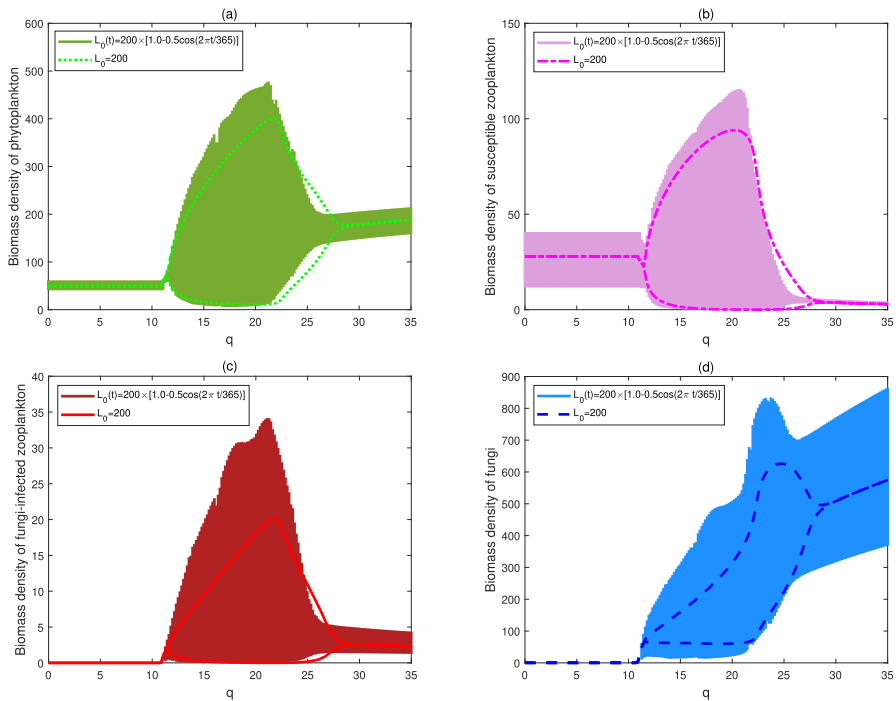


Fig. 10 Influence of maximal spore yield q under constant or seasonal light intensity

and seasonal light intensity on population dynamics. Comparing these bifurcation diagrams, one can see that the dynamics of the seasonal light intensity model are similar to those of the constant light intensity model. The difference is that under constant light intensity, the solution of the system converges to a positive stable equilibrium or a positive periodic solution as the parameter β changes. The seasonal light intensity is the cosine disturbance added to the constant light intensity. In this case, the biomass of all populations is always in an oscillatory state. This shows that seasonal light intensity brings greater uncertainty to the population.

We now explore the effects of fungal parasite transmission on phytoplankton biomass by comparing systems with and without fungal parasites. Compare Fig. 11a with b, it can be seen that the presence of fungal parasites reduces zooplankton biomass (the combined amount of susceptible and infected zooplankton) and increases the phytoplankton biomass. This study confirms that fungal parasites are beneficial to the increase of phytoplankton biomass.

5 Discussion

The fungal parasite is an important component of aquatic communities. They parasitize on zooplankton for their survival and reproduction (Hall et al. 2009; Shocket et al. 2018; Strauss et al. 2015; Cáceres et al. 2014; Civitello et al. 2013). They replicate and

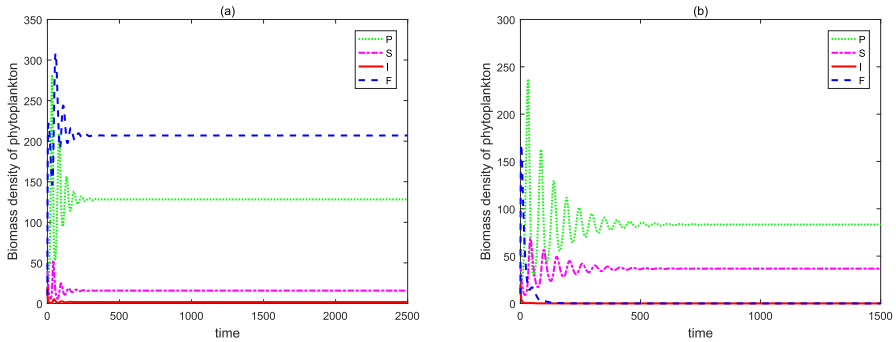


Fig. 11 Time series diagrams for phytoplankton biomass. (a) Time series diagram with fungal parasite transmission ($d_f = 0.04$). (b) Time series plot without fungal parasite transmission ($d_f = 0.13$). Here $L_0 = 500$, $N_0 = 110$, $d_p = 0.06$, $a = 0.003$, $\beta = 0.1$, $q = 25$

reproduce inside zooplankton, and finally release fungal spores after the zooplankton dies. The host zooplankton feed on phytoplankton. The release of fungal spores also depends on phytoplankton biomass. Few mathematical models have been formulated to explore the mechanisms of fungal parasite transmission among zooplankton and investigate the relationship between fungal parasite transmission and phytoplankton blooms.

A dynamical model (1) was proposed to describe the spread of fungal parasites among zooplankton in a planktonic ecosystem. Compared with the existing models in Cáceres et al. (2014), Shocket et al. (2018), and Strauss et al. (2015), there are three novel points in model (1). The first is to incorporate the fact that phytoplankton growth requires both light and nutrients. The second is to provide the basic reproduction number for fungal parasite transmission through rigorous theoretical analysis. The third is to take into account the influence of variable light intensity L_0 and nutrient input concentration N_0 , and how changes in light intensity affect the model. The findings demonstrate that light and nutrients have significant effects on the spread of fungal parasites and phytoplankton biomass.

We rigorously obtained the basic reproductive number, R_0 , for the spread of the fungal parasites from the model (1). According to Theorems 3.2-3.6, if $d_p > d_p^*$, all populations go extinct; if $d_p < d_p^*$ and $d_z > d_z^*$, the invasion of phytoplankton will be successful, while zooplankton and fungal parasites go extinct; if $d_p < \bar{d}_p$ and $R_0 < 1$, both phytoplankton and zooplankton successfully invade, while fungal parasites go extinct; if $R_0 > 1$ and $0 < d_f < d_f^*$, the fungal parasites spread among zooplankton. Based on theoretical and numerical analysis of model (1), we investigated the effect of ecological factors on fungal parasite transmission and explored the interaction between fungal parasite transmission and phytoplankton blooms. From Fig. 2, we can observe that an increase in the parameters β , q , L_0 , N_0 and δ promotes the spread of fungal parasites. Conversely, an increase in the parameters x_l and l_0 inhibits the spread of fungal parasites. From bifurcation diagrams Figs. 5 and 7, one can see that fungal epidemics are difficult to spread in low-light or oligotrophic aquatic environments. Based on bifurcation diagrams of β and q , we find that the dynamics of model (1) under

constant light intensity are similar to those under seasonal light intensity (Fig. 9a–d and Fig. 10 a–d). These results indicate that the spread of fungal parasites increases phytoplankton production and induces blooms (Fig. 11).

Compared to the existing research, our model considers the effects of light and nutrients on the spread of fungal parasites. This consideration makes the system more complex. It is difficult for us to analyze the complete dynamics of the model (1). We currently cannot resolve the global dynamic properties of (1), such as the global asymptotic stability of E_1 and E_2 and the uniqueness and stability of E_3 . This is an interesting problem that we will consider next. Our work assumes that the nutrient-to-carbon ratio in phytoplankton cells is constant, but in reality, this ratio is variable (Wang et al. 2007; Loladze et al. 2000). Therefore, it is necessary to incorporate stoichiometry into the model. In this work, we only consider the fungi *Metschnikowia bicuspidata* that only parasitizes zooplankton. However, fungal parasites can also infect phytoplankton, such as Chytridiomycota. It is of great interest to explore the spread of these fungal parasites among phytoplankton.

Appendix A Proof of Theorem 3.1

It follows from model (1) that

$$\frac{dN}{dt} \leq \frac{D}{x_l}(N_0 - N),$$

and then

$$\limsup_{t \rightarrow \infty} N(t) \leq N_0. \tag{10}$$

It follows from the P equations in (1) that

$$\frac{dP}{dt} \leq (rg(N_0)f(P) - d_p) P$$

for sufficiently large t . This means that

$$\limsup_{t \rightarrow \infty} P(t) \leq A,$$

where A satisfies

$$rg(N_0)f(A) = d_p.$$

From the first, second and third equations of (1), one can verify that

$$\begin{aligned} \frac{d(eP + S + I)}{dt} &= erg(N)f(P)P - d_p eP - d_z(S + I) - \delta I - (1 - \rho)\pi_1(P)I \\ &\leq erg(N_0)f(0)A - \min\{d_p, d_z\}(eP + S + I) \end{aligned}$$

for sufficiently large t . According to the comparison theorem, we obtain

$$\limsup_{t \rightarrow \infty} (eP + S + I)(t) \leq \frac{erg(N_0)f(0)A}{\min\{d_p, d_z\}}.$$

From the fourth equation of (1), one has

$$\frac{dF}{dt} \leq \delta\sigma(A)B - d_f F$$

for sufficiently large t , and then

$$\limsup_{t \rightarrow \infty} F(t) \leq \frac{\sigma(A)\delta B}{d_f}.$$

This means that the set Δ is a globally attracting region and system (1) is dissipative.

Appendix B Proofs of Existence and Stability Results

Appendix B.1 Proof of Theorem 3.2

It is obvious that $E_0 \equiv (0, 0, 0, 0, N_0)$ always exists and is unique. The Jacobian matrix evaluated at E_0 is

$$J(E_0) = \begin{pmatrix} rg(N_0)f(0) - d_p & 0 & 0 & 0 & 0 \\ 0 & -d_z & 0 & 0 & 0 \\ 0 & 0 & -d_z - \delta & 0 & 0 \\ 0 & 0 & 0 & -d_p & 0 \\ -c_p rg(N_0)f(0) & 0 & 0 & 0 & -\frac{D}{x_l} \end{pmatrix},$$

which has five eigenvalues: $\lambda_1 = -d_z < 0$, $\lambda_2 = -d_z - \delta < 0$, $\lambda_3 = -d_p < 0$, $\lambda_4 = -D/x_l < 0$, $\lambda_5 = rg(N_0)f(0) - d_p$. Note that $rg(N_0)f(0) - d_p < 0$ if $d_p > d_p^*$, thus, all the eigenvalues of $J(E_0)$ have negative real parts. This suggests that E_0 is locally asymptotically stable if $d_p > d_p^*$. Conversely, if $d_p < d_p^*$, then E_0 is unstable.

Next, we show that E_0 is globally asymptotically stable. From (10) and the first equation of (1), one has

$$\frac{dP}{dt} \leq (rg(N_0)f(0) - d_p)P$$

for sufficiently large t , then

$$\limsup_{t \rightarrow \infty} P(t) = 0,$$

if $d_p > d_p^*$ holds. From the theory of asymptotical autonomous systems (Mischaikow et al. 1995), the second and fourth equations in (1) reduce to

$$\begin{aligned} \frac{dS}{dt} &= -d_z S - \beta a F S, \\ \frac{dF}{dt} &= -d_f F - a F (S + I), \end{aligned} \tag{11}$$

which imply that

$$\limsup_{t \rightarrow \infty} S(t) = 0 \text{ and } \limsup_{t \rightarrow \infty} F(t) = 0.$$

Following similar arguments as above, we obtain

$$\limsup_{t \rightarrow \infty} I(t) = 0.$$

It follows from the theory of asymptotical autonomous systems (see (Mischaikow et al. 1995)) that (1) reduces to

$$\frac{dN}{dt} = \frac{D}{x_l} (N_0 - N).$$

This implies that

$$\lim_{t \rightarrow \infty} N(t) = N_0,$$

and E_0 is globally attractive. Then E_0 is globally asymptotically stable.

Appendix B.2 Proof of Theorem 3.3

Using a proof similar to Theorem 3.3 in Chen et al. (2022), it follows that E_1 exists and is unique, if $d_p < d_p^*$.

Next, we show that E_1 is locally asymptotically stable. The Jacobian matrix at E_1 is

$$J(E_1) = \begin{pmatrix} a_{11} & a_{12} & a_{13} & 0 & a_{15} \\ 0 & a_{22} & a_{23} & 0 & 0 \\ 0 & 0 & a_{33} & 0 & 0 \\ 0 & 0 & a_{43} & a_{44} & 0 \\ a_{51} & 0 & 0 & 0 & a_{55} \end{pmatrix},$$

where

$$a_{11} = rg(N_1)f'(P_1)P_1, \quad a_{12} = -aP_1, \quad a_{13} = -aP_1, \quad a_{15} = rg'(N_1)f(P_1)P_1,$$

$$\begin{aligned}
 a_{22} &= eaP_1 - d_z, \quad a_{23} = eaP_1, \quad a_{33} = -d_z - \delta, \quad a_{43} = \delta \frac{qP_1}{h_1 + P_1}, \\
 a_{44} &= -d_f, \quad a_{51} = -c_p r g(N_1) f(P_1) - c_p r g(N_1) f'(P_1) P_1, \\
 a_{55} &= -\frac{D}{x_l} - c_p r g'(N_1) f(P_1) P_1.
 \end{aligned}$$

$J(E_1)$ has eigenvalues $\lambda_1 = -d_z - \delta < 0$, $\lambda_2 = -d_f < 0$, $\lambda_3 = eaP_1 - d_z := d_z^* - d_z$, and the other two eigenvalues satisfy $|\lambda I - M| = 0$, where

$$M = \begin{pmatrix} a_{11} & a_{15} \\ a_{51} & a_{55} \end{pmatrix}.$$

Given that the function f monotonically decreases with respect to P , and that g monotonically increases with respect to N , a straightforward computation yields

$$\begin{aligned}
 \text{Det}M &= -r g(N_1) f'(P_1) P_1 D/x_l + c_p r^2 f^2(P_1) g'(N) g(N_1) P_1 > 0, \\
 \text{Tr}M &= r g(N_1) f'(P_1) P_1 - D/x_l - c_p r g'(N_1) f(P_1) P_1 < 0.
 \end{aligned} \tag{12}$$

Thus E_1 is locally asymptotically stable provided that $d_z > d_z^*$. If $d_z < d_z^*$, then at least one eigenvalue is positive and hence E_1 is unstable.

Appendix B.3 Proof of Theorem 3.5

We first prove the existence of disease-free equilibrium of (1). From (5), we get $P_2 = \frac{d_z}{ea} > 0$. Substituting P_2 into (6) yields

$$N_2 = \frac{\sqrt{(c_p r f(P_2) P_2 x_l + D(\gamma - N_0))^2 + 4\gamma D^2 N_0} - (c_p r f(P_2) P_2 x_l + D(\gamma - N_0))}{2D} > 0.$$

By substituting the expressions for N_2 and P_2 into equation (4), we obtain

$$S_2 = \frac{r g(N_2) f(P_2) - d_p}{a}.$$

Note that $S_2 > 0$ if $d_p < \bar{d}_p$. This indicates that E_2 exists when $d_p < \bar{d}_p$.

We then show that E_2 is locally asymptotically stable. The Jacobian matrix at E_2 is

$$J(E_2) = \begin{pmatrix} a_{11} & a_{12} & a_{13} & 0 & a_{15} \\ a_{21} & 0 & a_{23} & a_{24} & 0 \\ 0 & 0 & a_{33} & a_{34} & 0 \\ 0 & 0 & a_{43} & a_{44} & 0 \\ a_{51} & 0 & 0 & 0 & a_{55} \end{pmatrix},$$

where

$$\begin{aligned}
 a_{11} &= rg(N_2)f'(P_2)P_2 - aS_2, \quad a_{12} = -aP_2, \quad a_{13} = -aP_2, \quad a_{15} = rg'(N_2)f(P_2)P_2, \\
 a_{21} &= eaS_2, \quad a_{23} = eaP_2, \quad a_{24} = -\beta aS_2, \\
 a_{33} &= -d_z - \delta, \quad a_{34} = \beta aS_2, \quad a_{43} = \delta\sigma(P_2), \quad a_{44} = -d_f - aS_2, \\
 a_{51} &= -c_p rg(N_2)f(P_2) - c_p rg(N_2)f'(P_2)P_2, \quad a_{55} = -D/x_l - c_p rg'(N_2)f(P_2)P_2.
 \end{aligned}$$

From the expression of $J(E_2)$, it is clear that $J(E_2)$ can be divided into two parts

$$J_1(E_2) := \begin{pmatrix} a_{11} & a_{12} & a_{15} \\ a_{21} & 0 & 0 \\ a_{51} & 0 & a_{55} \end{pmatrix}, \quad \text{and } J_2(E_2) := \begin{pmatrix} a_{33} & a_{34} \\ a_{43} & a_{44} \end{pmatrix}.$$

The characteristic equation of $J_1(E_2)$ is

$$\lambda^3 + C_1\lambda^2 + C_2\lambda + C_3 = 0,$$

where

$$\begin{aligned}
 C_1 &= -rg(N_2)f'(P_2)P_2 + aS_2 + D/x_l + c_p rg'(N_2)f(P_2)P_2, \\
 C_2 &= ea^2P_2S_2 + c_p r^2 f^2(P_2)g(N_2)g'(N_2)P_2 \\
 &\quad + (rg(N_2)f'(P_2)P_2 - aS_2)(-D/x_l) + ac_p rf(P_2)g'(N_2)P_2S_2, \\
 C_3 &= ea^2P_2S_2(D/x_l + c_p rg'(N_2)f(P_2)P_2).
 \end{aligned}$$

Based on the monotonicity of the functions f and g , we have $C_1, C_2, C_3 > 0$ and $C_1C_2 - C_3 > 0$. Thus, three eigenvalues of $J_1(E_2)$ have negative real parts. Furthermore, it's clear that $\text{Tr}(J_2(E_2)) = a_{33} + a_{44} < 0$ and $\text{Det}(J_2(E_2)) = a_{33}a_{44} - a_{34}a_{43} > 0$, if $R_0 < 1$. Hence, the two eigenvalues of $J_2(E_2)$ have negative real parts. E_2 is locally asymptotically stable if $R_0 < 1$.

Appendix B.4 Proof of Theorem 3.6

The proof is divided into two parts, local bifurcation and global bifurcation.

(i) Local bifurcation. Define a mapping $W : \mathbb{R}^+ \times \mathbb{R}^5 \rightarrow \mathbb{R}^5$ by

$$W(d_f, P, S, I, F, N) = \begin{pmatrix} rg(N)f(P)P - d_p P - \pi_1(P)(S + I) \\ e\pi_1(P)(S + I) - d_z S - \beta\pi_2(F)S \\ \beta\pi_2(F)S - d_z I - \delta I \\ \delta\sigma(P)I - d_f F - \pi_2(F)(S + I) \\ \frac{D}{x_l}(N_0 - N) - c_p rg(N)f(P)P \end{pmatrix}.$$

Obviously, $W(d_f, P_2, S_2, 0, 0, N_2) = 0$. Let $H := W_{(P,S,I,F,N)}(d_f^*, P_2, S_2, 0, 0, N_2)$. We have

$$H[\xi_1, \xi_2, \xi_3, \xi_4, \xi_5] = \begin{pmatrix} h_1(\xi_1, \xi_3, \xi_5) \\ h_2(\xi_1, \xi_3, \xi_4) \\ h_3(\xi_3, \xi_4) \\ h_4(\xi_3, \xi_4) \\ h_5(\xi_1, \xi_5) \end{pmatrix},$$

for any $(\xi_1, \xi_2, \xi_3, \xi_4, \xi_5) \in \mathbb{R}_+^5$, where

$$\begin{aligned} h_1 &= (rg(N_2)f'(P_2)P_2 - aS_2)\xi_1 - aP_2\xi_2 - aP_2\xi_3 + rg'(N_2)f(P_2)P_2\xi_5, \\ h_2 &= eaS_2\xi_1 + e\pi(P_2)\xi_3 - \beta aS_2\xi_4, \\ h_3 &= -(d_z + \delta)\xi_3 + \beta aS_2\xi_4, \\ h_4 &= \sigma(P_2)\delta\xi_3 - (d_f^* + \beta aS_2)\xi_4, \\ h_5 &= -(c_p rg(N_2)f(P_2) + c_p rg(N_2)f'(P_2)P_2)\xi_1 - \left(\frac{D}{x_l} + c_p rg'(N_2)f(P_2)P_2\right)\xi_5. \end{aligned}$$

For $(\xi_1, \xi_2, \xi_3, \xi_4, \xi_5) \in \ker H$, one can obtain

$$h_i = 0, i = 1, 2, 3, 4, 5. \tag{13}$$

From $d_f^* = aS_2 \left(\frac{\beta\sigma(P_2)\delta}{\delta+d_z} - 1 \right)$, we have $h_3 = h_4$ and

$$\xi_3 = -\frac{aS_2}{\delta\sigma(P_2)} \left(\beta \left(1 + \frac{\delta\sigma(P_2)}{d_z + \delta} \right) - 1 \right) \xi_4.$$

Let $\xi_4 = 1$, then it is clear that (13) has a unique solution $(\hat{\xi}_1, \hat{\xi}_2, \hat{\xi}_3, 1, \hat{\xi}_5)$. Then $\dim \ker H = 1$, $\ker H = \text{span}(\hat{\xi}_1, \hat{\xi}_2, \hat{\xi}_3, 1, \hat{\xi}_5)$. Hence

$$\text{range } H = \{(\sigma_1, \sigma_2, \sigma_3, \sigma_4, \sigma_5) \in \mathbb{R}^5 : \sigma_3 = \sigma_4\},$$

then $\text{codim range } F = 1$. A direct calculation gives

$$H_{d_f(P,S,I,F,N)}(d_f^*, P_2, S_2, 0, 0, N_2)(\hat{\xi}_1, \hat{\xi}_2, \hat{\xi}_3, 1, \hat{\xi}_5) = (0, 0, 0, -1, 0) \notin \text{range } P.$$

Based on the Crandall-Rabinowitz bifurcation theorem (Crandall and Rabinowitz 1971), Theorem 1.7), all positive solutions of (1) near $(d_f^*, P_2, S_2, 0, 0, N_2)$ are on a smooth curve

$$\Gamma = \{(d_f(s), P_3(s), S_3(s), I_3(s), F_3(s), N_3(s)) : 0 < s < \varepsilon\},$$

for some $\varepsilon > 0$ with the form

$$\begin{aligned} P_3(s) &= P_2 + s\hat{\xi}_1 + o(s), \quad S_3(s) = S_2 + s\hat{\xi}_2 + o(s), \quad I_3(s) = s + o(s), \\ F_3(s) &= s + o(s), \quad N_3(s) = N_2 + s\hat{\xi}_5 + o(s). \end{aligned} \tag{14}$$

(ii) Global bifurcation. Let Υ be the set of all positive coexistence equilibria of (1). It follows from Theorem 3.3 and Remark 3.4 in Shi and Wang (2009), there exists a connected component Υ^+ of Υ such that it includes Γ , and its closure contains the bifurcation point $(d_f^*, P_2, S_2, 0, 0, N_2)$. Moreover, Υ^+ has one of the following three cases:

- (1) it is not compact in $\mathbb{R}^+ \times \mathbb{R}^5$,
- (2) it meets another bifurcation point $(\tilde{d}_f, P_2, S_2, 0, 0, N_2)$ with $\tilde{d}_f \neq d_f^*$,
- (3) it contains $(d_f, P_2 + \hat{P}_3, S_2 + \hat{S}_3, \hat{I}_3, \hat{F}_3, N_2 + \hat{N}_3)$ with $0 \neq (\hat{P}_3, \hat{S}_3, \hat{I}_3, \hat{F}_3, \hat{N}_3) \in \mathbb{X}$, where \mathbb{X} is a closed complement of $\ker H = \text{span}\{\hat{\eta}_1, \hat{\eta}_2, \hat{\eta}_3, 1, \hat{\eta}_5\}$ in \mathbb{R}_+^5 .

If the case (3) occurs, then $\hat{I}_3 = \hat{F}_3 = 0$, which is a contradiction to $\hat{I}_3, \hat{F}_3 > 0$ since it is a positive steady state. If (2) holds and \tilde{d}_f is another bifurcation value from Γ . Hence, there exists a positive coexistence steady state sequence $\{(d_f^n, P_3^n, S_3^n, I_3^n, F_3^n, N_3^n)\}$ satisfying

$$\{(d_f^n, P_3^n, S_3^n, I_3^n, F_3^n, N_3^n)\} \rightarrow \{(d_f^*, P_2^n, S_2^n, 0, 0, N_2^n)\}$$

as $n \rightarrow \infty$. From the third and fourth equations in (1), we have

$$\begin{aligned} \beta a F_3^n S_3^n - d_z I_3^n - \delta I_3^n &= 0, \\ \sigma(P_3^n) \delta I_3^n - d_f^n F_3^n - \beta a F_3^n (S_3^n + I_3^n) &= 0. \end{aligned} \tag{15}$$

From the first equation of (15), we obtain

$$I_3^n = \frac{\beta a F_3^n S_3^n}{d_z + \delta}.$$

Substituting this into the second equation of (15), we have

$$\delta \sigma(P_3^n) \frac{\beta a S_3^n}{d_z + \delta} - d_f^n - a(S_3^n + \frac{\beta a F_3^n S_3^n}{d_z + \delta}) = 0.$$

Hence

$$\delta \sigma(P_2) \frac{\beta a S_2}{d_z + \delta} - \tilde{d}_f - a S_2 = 0,$$

when $n \rightarrow \infty$, which means that $\tilde{d}_f = d_f^*$. The above discussion indicates that (1) must hold. Then Υ^+ is not compact in \mathbb{R}^6 . It follows from Theorem 3.1 that

$$N \leq N_0, \quad (eP + S + I) \leq \frac{\text{erg}(N_0) f(0) A}{\min\{d_p, d_z\}}, \quad F \leq \frac{\sigma(A) \delta B_1}{d_f},$$

for all $d_f \in (0, d_f^*)$. This indicates that the projection of Υ^+ onto d_f -axis contains $(0, d_f^*)$. The proof is complete.

Author Contributions Y.Y. developed and analyzed the mathematical models, realized numerical simulations, and wrote the manuscript. J.J. and H.W. supervised this work. All authors wrote and reviewed the manuscript.

Funding Yan is supported by HEU PhD Scholarship; Ji is supported by National Natural Science Foundation of P. R. China (No. 12401635); Wang is supported by the Natural Sciences and Engineering Research Council of Canada (Individual Discovery Grant RGPIN-2020-03911 and Discovery Accelerator Supplement Award RGPAS-2020-00090).

Availability of data and materials Not applicable.

Declarations

Conflict of interest The authors declare that they have no Conflict of interest.

Ethical Approval Not applicable.

References

- Cáceres CE, Davis G, Duple S, Hall SR, Koss A, Lee P, Rapti Z (2014) Complex daphnia interactions with parasites and competitors. *Math Biosci* 258:148–161. <https://doi.org/10.1016/j.mbs.2014.10.002>
- Chen LF, Yu XW, Yuan SL (2022) Effects of random environmental perturbation on the dynamics of a nutrient-phytoplankton-zooplankton model with nutrient recycling. *Mathematics* 10(20):3783. <https://doi.org/10.3390/math10203783>
- Chen M, Fan M, Kuang Y (2017) Global dynamics in a stoichiometric food chain model with two limiting nutrients. *Math Biosci* 289:9–19. <https://doi.org/10.1016/j.mbs.2017.04.004>
- Chen Ming, Gao Honghui, Zhang Jimin (2024) Mycoloop: Modeling phytoplankton–chytrid–zooplankton interactions in aquatic food webs. *Mathematical Biosciences* 368:109134. <https://doi.org/10.1016/j.mbs.2023.109134>
- Chen M, Zhang JM, Ejegul S (2022) Dynamics of autotroph-mixotroph interactions with the intraguild predation structure. *J Biol Dynam* 16(1):186–206. <https://doi.org/10.1080/17513758.2022.2066729>
- Civitello DJ, Pearsall S, Duffy MA, Hall SR (2013) Parasite consumption and host interference can inhibit disease spread in dense populations. *Ecol Lett* 16(5):626–634. <https://doi.org/10.1111/ele.12089>
- Crandall MG, Rabinowitz PH (1971) Bifurcation from simple eigenvalues. *J Funct Anal* 8(2):321–340. [https://doi.org/10.1016/0022-1236\(71\)90015-2](https://doi.org/10.1016/0022-1236(71)90015-2)
- Davies CM, Wang H (2021) Incorporating carbon dioxide into a stoichiometric producer-grazer model. *J Math Biol* 83(5):49. <https://doi.org/10.1007/s00285-021-01658-3>
- Hall SR, Simonis JL, Nisbet RM, Tessier AJ, Cáceres CE (2009) Resource ecology of virulence in a planktonic host-parasite system: an explanation using dynamic energy budgets. *Am Nat* 174(2):149–162. <https://doi.org/10.1086/600086>
- Hall SR, Sivers-Becker L, Becker C, Duffy MA, Tessier AJ, Cáceres CE (2007) Eating yourself sick: transmission of disease as a function of foraging ecology. *Ecol Lett* 10(3):207–218. <https://doi.org/10.1111/j.1461-0248.2007.01011.x>
- Huisman Jef, Pham Thi Nga N., Karl David M., Sommeijer Ben (2006) Reduced mixing generates oscillations and chaos in the oceanic deep chlorophyll maximum. *Nature* 439(7074):322–325. <https://doi.org/10.1038/nature04245>
- Huisman J, Weissing FJ (1994) Light-limited growth and competition for light in well-mixed aquatic environments: an elementary model. *Ecology* 75(2):507–520. <https://doi.org/10.1111/j.1461-0248.2007.01011.x>

- Kagami M, de Bruin A, Ibelings BW, Van Donk E (2007) Parasitic chytrids: their effects on phytoplankton communities and food-web dynamics. *Hydrobiologia* 578:113–129. <https://doi.org/10.1007/s10750-006-0438-z>
- Klausmeier CA, Litchman E (2001) Algal games: The vertical distribution of phytoplankton in poorly mixed water columns. *Limnol Oceanogr* 46(8):1998–2007. <https://doi.org/10.4319/lo.2001.46.8.1998>
- Loladze I, Kuang Y, Elser JJ (2000) Stoichiometry in producer–grazer systems: linking energy flow with element cycling. *Bull Math Biol* 62(6):1137–1162. <https://doi.org/10.1006/bulm.2000.0201>
- Mischaikow K, Smith HL, Thieme HR (1995) Asymptotically autonomous semiflows: chain recurrence and lyapunov functions. *Trans Am Math Soc* 347(5):1669–1685. <https://doi.org/10.1090/S0002-9947-1995-1290727-7>
- Müller-Navarra DC, Brett MT, Liston AM, Goldman CR (2000) A highly unsaturated fatty acid predicts carbon transfer between primary producers and consumers. *Nature* 403(6765):74–77. <https://doi.org/10.1038/nature02210>
- Pang DF, Nie H, Wu JH (2019) Single phytoplankton species growth with light and crowding effect in a water column. *Discrete Contin Dyn Syst* 39:41–74. <https://doi.org/10.3934/dcds.2019003>
- Peace A (2015) Effects of light, nutrients, and food chain length on trophic efficiencies in simple stoichiometric aquatic food chain models. *Ecol Modell* 312:125–135. <https://doi.org/10.1016/j.ecolmodel.2015.05.019>
- Peng R, Zhao XQ (2016) A nonlocal and periodic reaction-diffusion-advection model of a single phytoplankton species. *J Math Biol* 72(3):755–791. <https://doi.org/10.1007/s00285-015-0904-1>
- Shi JP, Wang XF (2009) On global bifurcation for quasilinear elliptic systems on bounded domains. *J Differ Equ* 246(7):2788–2812. <https://doi.org/10.1016/j.jde.2008.09.009>
- Shocket MS, Strauss AT, Hite JL, Šljivar M, Civitello DJ, Duffy MA, Cáceres CE, Hall SR (2018) Temperature drives epidemics in a zooplankton-fungus disease system: A trait-driven approach points to transmission via host foraging. *Am Nat* 191(4):435–451
- Strauss AT, Civitello DJ, Cáceres CE, Hall SR (2015) Success, failure and ambiguity of the dilution effect among competitors. *Ecol Lett* 18(9):916–926. <https://doi.org/10.1111/ele.12468>
- Van den Driessche P, Watmough J (2002) Reproduction numbers and sub-threshold endemic equilibria for compartmental models of disease transmission. *Math Biosci* 180(1–2):29–48. [https://doi.org/10.1016/S0025-5564\(02\)00108-6](https://doi.org/10.1016/S0025-5564(02)00108-6)
- Wang H, Smith HL, Kuang Y, Elser JJ (2007) Dynamics of stoichiometric bacteria-algae interactions in the epilimnion. *SIAM J Appl Math* 68(2):503–522. <https://doi.org/10.1137/060665919>
- Yan YW, Zhang JM, Wang H (2022) Algae-bacteria interactions with nutrients and light: A reaction-diffusion-advection model. *J Nonlinear Sci* 32(4):56. <https://doi.org/10.1007/s00332-022-09815-8>
- Yan YW, Zhang JM, Wang H (2022) Dynamics of stoichiometric autotroph-mixotroph-bacteria interactions in the epilimnion. *Bull Math Biol* 84:1–30. <https://doi.org/10.1007/s11538-021-00962-9>
- Yu XW, Yuan SL, Zhang TH (2019) Asymptotic properties of stochastic nutrient-plankton food chain models with nutrient recycling. *Nonlinear Anal-hybr* 34:209–225. <https://doi.org/10.1016/j.nahs.2019.06.005>
- Zhang JM, Cong PP, Fan M (2023) Interactions between pelagic and benthic producers: asymmetric competition for light and nutrients. *SIAM J Appl Math* 83(2):530–552. <https://doi.org/10.1137/22M1491290>
- Zhao SN, Yuan SL, Wang H (2020) Threshold behavior in a stochastic algal growth model with stoichiometric constraints and seasonal variation. *J Differ Equ* 268(9):5113–5139. <https://doi.org/10.1016/j.jde.2019.11.004>

Publisher's Note Springer Nature remains neutral with regard to jurisdictional claims in published maps and institutional affiliations.

Springer Nature or its licensor (e.g. a society or other partner) holds exclusive rights to this article under a publishing agreement with the author(s) or other rightsholder(s); author self-archiving of the accepted manuscript version of this article is solely governed by the terms of such publishing agreement and applicable law.